

# A random rule model of surface growth

Bernardo A. Mello\*

*Physics Institute, University of Brasilia, 70919-970, Brasilia, Brazil*

---

## Abstract

Stochastic models of surface growth are usually based on randomly choosing a substrate site to perform iterative steps, as in the etching model [1]. In this paper I modify the etching model to perform sequential, instead of random, substrate scan. The randomness is introduced not in the site selection but in the choice of the rule to be followed in each site. The change positively affects the study of dynamic and asymptotic properties, by reducing the finite size effect and the short-time anomaly and by increasing the saturation time. It also has computational benefits: better use of the cache memory and the possibility of parallel implementation.

Published as: *Physica A* 419 (2015) 762767

DOI: 10.1016/j.physa.2014.10.064

**Keywords:** Stochastic surface models, etching model, short time anomaly, finite length effect

---

## 1. Introduction

Stochastic simulation of surface growth plays a major role in the studies of fractal surface dynamics. The first model of this kind, ballistic deposition, was presented in 1959 [2]. A key aspect of that model is the random choice of sites for the deposition of new atoms.

Since then, several models have been proposed combining the random site selection with a relaxation mechanism. Among them is the Eden model [3], random deposition with surface relaxation [4] the restricted solid on solid model [5] and the etching model [1].

Simulations performed with those models have made important contributions to the field, but randomly accessing the surface elements impairs the benefits from two main advances of modern computers: cache memory and parallelism on multiple cores of CPUs and graphics processing units (GPUs). The reasons for that are discussed later.

---

\*Email address: bernardo@fis.unb.br

In this work I propose an alternative way of inserting randomness into surface dynamics. Instead of randomly choosing the *position*, the substrate is sequentially swept and the *rule* followed in each site is randomly chosen. Composed of clearly separated rules, the etching model is particularly suitable for this approach.

Another model that introduces sequential sweeping is synchronous ballistic deposition [6], but in that model the rule is always the same and the stochasticity comes from the rule being applied or not with a given probability.

## 2. Three Versions of the Etching Model

The etching model, which in this paper it will be called the *random site etching* (RSE), was introduced in 2001 to simulate the removal of atoms in a square lattice. Simulations based on this model have been used to explore several aspects of fractal surface dynamics [7, 8, 9, 10, 11, 12, 13, 14, 15, 16].

The probability of an atom being removed in the RSE is proportional to the number of exposed faces of that atom. The higher etching probability of the more exposed atoms may be justified either by the bigger area available to the etching agent or by the lower number of chemical bounds between the atom and the substrate.

Despite its introduction as a model of etching, the RSE can also be seen as a deposition process where the probability that an atom attaches to a site is proportional to the number of bounds that will be formed between the new atom and the ones already in the substrate. Discussion in this paper are mostly based in this interpretation.

Whatever the interpretation, the etching model is usually implemented with the surface moving towards positive height, as if it was deposition from above or etching from below. The iterative procedure of the one-dimensional version of the RSE is:

- randomly chooses  $i \in \{1, \dots, L\}$ ;
- if  $h_{i+\delta} < h_i$ , do  $h_{i+\delta} = h_i$ , with  $\delta = \pm 1$ ;
- $h_i = h_i + 1$ .

In the  $d$ -dimensional case,  $i$  and  $\delta$  are vectors and  $\delta$  runs over the  $2^d$  first neighbors. If  $L$  is the substrate length along each direction, the total number of sites is  $L^d$ . With the time unit defined as the average time of one deposition at each exposed face, one iteration corresponds to the advance of  $1/L^d$  in time.

Careful analysis of the RSE algorithm reveal that the deposition of one atom is proportional to the number of the neighbors it will have. The model I presented below keeps this property but affect only the atom  $i$ , preserving the state of the neighbors. This model will be called *random rule etching* (RRE) to clearly distinguish it from the original *random site etching* (RSE).

While the iterative update of RSE is performed in the same data structure  $h$ , the RAE require two such structures,  $h^1$  and  $h^0$ , therefore using twice as much memory.

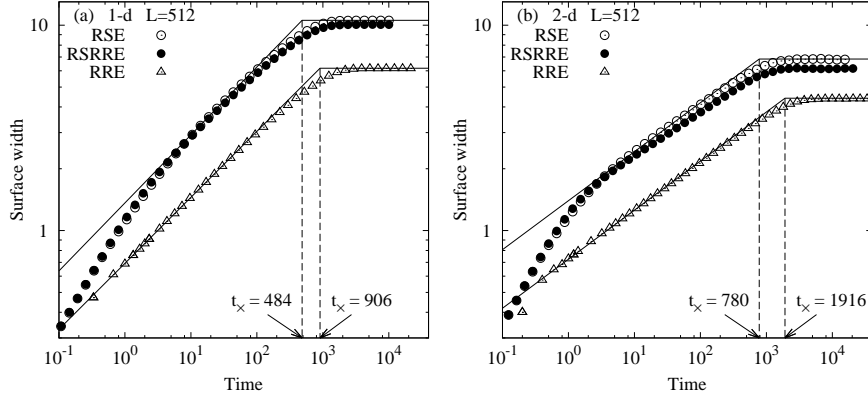


Figure 1: Surface width as a function of time for a) one-dimensional and b) two-dimensional substrates with  $L = 512$ . If different values of  $L$  are used, the data points within each dimension are identical for  $t \ll t_x$ .

In the RRE the substrate is sequentially accessed and for each site  $i \in \{1, \dots, L\}$  of the one-dimensional surface the following steps are performed

- randomly chooses  $\delta \in \{-1, 0, 1\}$ ;
- if  $\delta = 0$  make  $h_i^1 = h_i^0 + 1$ ;  
otherwise make  $h_i^1 = \max(h_i^0, h_{i+\delta}^0)$ .

After sweeping the lattice,  $h_0$  is replaced by  $h_1$ . In the  $d$ -dimensional case  $\delta \in [-d, \dots, d]$ . The neighbor to appear in the max function is located along the direction indicated by the modulus of  $\delta$ . There are two neighbors along each direction, discriminated by the sign of  $\delta$ . Each RSE iteration performs the  $2d + 1$  possible rules of the RRE, therefore, one RSE step corresponds to  $2d + 1$  RRE steps. A complete RRE substrate scan corresponds to the advance of  $1/(2d + 1)$  in time.

For the only reason of exploring the effects of randomness either in site selection or in the rule selection I define the *random site random rule etching* (RSRRE) model. This consists of the RRE with random, instead of sequential, site choosing.

### 3. Results and Discussion

According to the Family-Vicsek scaling relation [17], the surface width depends on  $t$  as a power law with exponent  $\beta$  for  $t \ll t_x$ , and saturates to  $w_s$  for  $t \gg t_x$ , as depicted in Figure 1. The values of  $w_s$  and  $t_x$  scales with  $L$  as, respectively,  $L^\alpha$  and  $L^z$ .

In Figure 1 a remarkable deviation from the power law is observed in the RSE at short times. Such anomaly is present in all models cited in the second

paragraph of this paper [18, 4, 5, 1]. It undermines the determination of the exponent  $\beta$  and any other quantity related to the roughening process.

The evolution of the surface width of RRE in the same figure shows a much smaller short time anomaly, either in one or in two dimensions. Similar results occur in higher dimensions. That result is striking since surface width  $w \ll 1$  at  $t \sim 1$  and barely one layer has being grown. It is worth remembering that the substrate is swapped  $2d+1$  times at each time unit, thought that property alone cannot explain the distinct behaviour, as discussed in the next paragraphs.

Determining the reason for the reduction in the short-time anomaly is an inescapable question, since it will help the improvement of other models. For that reason simulations were conducted with the RSRRE model. In Figure 1 one can observe that the surface width evolution of that model is almost exactly the same as that of the RSE. Therefore, if the site is randomly chosen, almost the same effects are observed with of the former celular automata (RSE) or the one presently proposed (RSRRE), being them equivalent in that context.

By comparing the three data sets of both graphs of Figure 1 we can conclude that the randomness in the site choosing is a major cause of the short-time anomaly.

Exploring the conceptual differences of the RSRRE and the RRE sheds light on the discussion, even if we fail to pinpoint which differences or how such differences are related to the short-time anomaly.

The RRE implies one rule application at each site during the time interval of  $1/(2d+1)$ . With the RSRRE a given site may be updated several times while some other sites may get no update at all. That higher uniformity of the sequential scan is responsible for the smaller surface width of the RRE, as compared to the RSE and to the RSRRE.

The implementation of sequential access to the substrate imposes the use of two data structures. Whereas each iteration of the random site corresponds to one simulation time step, as in [6], all application of the rule performed during one sequential scan of the substrate happens at the same simulation time step. Since causal connection cannot exist among these simultaneous rule applications, information takes longer to travel the sequentially scanned substrate.

Another difference among the curves of Figure 1 is the value of  $t_\times$ , which is bigger for RRE. This fact, together with the minute short-time anomaly, leads to a better fitting of the power law to the RRE data of surface width evolution as compared to the RSE with the same substrate size. Consequently determining RRE's  $\beta$  demands smaller substrate than the RSE. This is particularly usefull when measuring the height distribution of in the growth region, currently an important point in the study of KPZ [19, 20, 21, 22, 23, 24, 25], or other studies of surface dynamic [26, 27]. To demonstrate it, I determined the exponents  $\alpha$  and  $\beta$  by following the procedure proposed in [28], described bellow.

For each value of  $L$ , linear regressions like those of figure 1, are done over the interval  $[t_{\min}, t_{\max}]$ . Considering the differences in the short-time anomalies, I adopted  $t_{\min} = 50$  for RSE and  $t_{\min} = 5$  for RRE, regardless the values of  $L$ .  $t_{\max}$  is the greatest value for which the Pearson correlation coefficient  $r < 0.9999$ . Figure 2a shows the dependence on  $L$  of the resulting regression

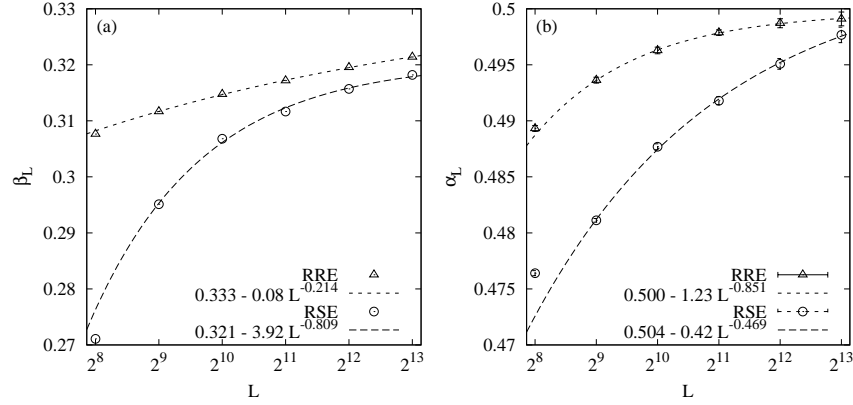


Figure 2: Dynamic exponents obtained from following the procedure described in [28] (see text). The fittings used the five rightmost points of each data set.

coefficient  $\beta_L$ .

The exponent  $\beta$  is the limit  $\beta_{L \rightarrow \infty}$ , which can be estimated from the fitting of equation

$$\beta_L \approx \beta + AL^{-\lambda}. \quad (1)$$

In Fig. 2a we can see the result of the fitting to the five rightmost points of each model. While the data points of RRE sit nicely on the curve, the same cannot be said of the RSE points. It indicates that bigger RSE substrates are required to obtain truthful values, as was done in [28], which went up to  $L = 16384$ . The resulting values of  $\beta$  are 0.321 and 0.333 for RSE and RRE, respectively, being  $1/3$  the value expected for a model belonging to the KPZ universality class.

For each size  $L$  the value of  $\alpha$  was obtained as

$$\alpha_L = \frac{1}{\log 2} \log \frac{w_s(L)}{w_s(L/2)}, \quad (2)$$

where  $w_s$  is the saturated width obtained at  $t \gg t_\times$ . Simulations were ran until the relative error of  $w_s$  be less the 0.1%. The value obtained are shown in Figure 2b. That exponent is not affected by the short-time anomaly but by the finite size effects [29]. From the faster convergence of the RRE as compared to RSE, for large values of  $L$ , we conclude that the finite size effects are smaller in RRE than in RSE. The asymptotic value  $\alpha = \alpha_L$  is obtained by doing the fitting to an equation equivalent to equation (1), resulting in  $\alpha = 0.504$  in RSE and  $\alpha = 0.500$  in RRE.

The exponents obtained in [28] for the RSE, using the same procedure, are  $\alpha = 0.507$  and  $\beta = 0.339$  in  $d = 1$  compatible with our results. For the RRE in  $d = 2$ , we found  $\alpha = 0.399$  and  $\beta = 0.242$ , while they found only  $\alpha = 0.360$ , for RSE, but suggested that the exact value should be  $\alpha = 0.4$ . These results suggest that both models belong to the same universality class in  $d = 1$  and  $d = 2$ .

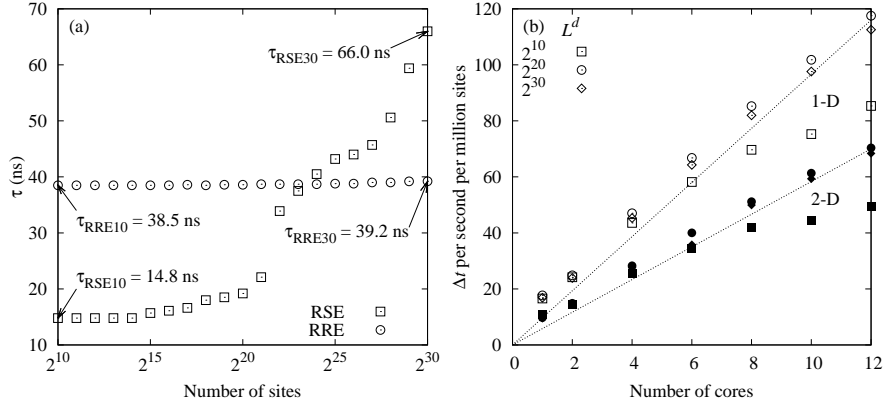


Figure 3: (a) CPU time ( $\tau$ ) of the stand alone simulation of one deposition of the etching model as function of the substrate size. Each site is stored as a 2 bytes integer in a computer with an Intel Core i5-2320 processor (6M cache, 3 GHZ) and 6 GB of memory. Similar curves were obtained in 2 and 3 dimensions. With  $d = 2$ ,  $\tau_{RSE10} = 24.1$  ns,  $\tau_{RSE30} = 127.8$  ns,  $\tau_{RRE10} = 61.6$  ns, and  $\tau_{RRE30} = 62.9$  ns. With  $d = 3$ ,  $\tau_{RSE12} = 34.6$  ns,  $\tau_{RSE30} = 172.3$  ns,  $\tau_{RRE12} = 85.0$  ns, and  $\tau_{RRE30} = 86.4$  ns. (b) The vertical axis represents the advance in time of the simulation of one million sites for one second of running. Hollow figures, one dimension, solid figures, two dimensions. Remember that each site is iterated  $2d + 1$  times at each time unit. Machine with two Intel Xeon X650 processors, each with 6 cores. The lines are only guides to the eyes.

Nevertheless, although both models express the same removal probability, the resulting dynamics are not exactly the same.

#### 4. Computational Benefits

Since modern CPUs are much faster than the access rate to the main memory, a small and fast memory, called cache, is used to keep the data which are being read or written by the CPU. Dedicated circuits try to anticipate the next segment of the main memory to be accessed and bring it to the cache before it is used. If data which is not already cached is requested, it must be fetched from the main memory, and the operation takes much longer than when the cache contains the data.

Programs that update data sequentially leads to a memory access pattern easily predicted by the cache managing circuit. Such applications may achieve an almost 100 % success rate in loading data to the cache before it is requested by the CPU.

The random choice of the deposition site present in most stochastic models of surface dynamics makes it impossible to anticipate which part of the memory will be accessed in the next iteration. This is not a serious problem when the whole substrate can be stored in the cache, however, it drastically degrades performance for bigger substrates. Computation time steps up when the used

memory  $2N_{\text{sites}} \approx 6\text{MB}$ , i.e., when  $N_{\text{sites}} \approx 10^{22}$ , as shown in Figure 3a. Complete understanding of how used memory affects the computation time requires the discussion of other optimization mechanisms, which is beyond the scope of this paper.

Figure 3a shows that the simulation time is almost constant for the RRE model, where the surface is sequentially scanned.

Another caveat of the random site selection is that the workload cannot be distributed among several processing units, each of them responsible for one sector of the substrate, as can be done in sequential access algorithms. This restriction prevents the use of computer parallelism in the evolution of one substrate. The limitation can be circumvented in multi-core computers by running independent substrates in each core, but the strategy cannot be used if the substrate size is comparable to the machine memory. In this case processing power will be wasted. Such situations occur when simulating high dimensionality substrates.

That drawback was made worse by the popularization of the use of graphic processing units (GPU) for scientific calculations, whose processing power may be more than a hundred times higher than that of desktop computers [30]. The gain is based on massive parallelism and GPUs may have hundreds or thousands of processing units with just a few gigabytes of memory. The ratio between processing power and memory size is much higher in the GPUs than in the conventional computers. This puts a more stringent limit on parallelism via the simulation of independent substrates.

Besides the sequential substrate scan, one important aspect of the RRE is that only the site  $i$  can be altered at each step, which makes code parallelization a simple task.

Once the RRE algorithm has been implemented, it can easily be parallelized to use the multiple cores of modern computers. One way of doing this in C or Fortran programs is by using openMP [31]. Each substrate scan is divided in  $N_T$  segments attributed to the  $N_T$  available threads. To improve efficiency,  $N_T$  independent<sup>1</sup> random generators must be created, each one used exclusively by a single thread. Care must be taken to avoid false sharing of the random generators and other variables private to the threads [32]. If properly implemented, good scalability is achieved for big substrates, as can be seen in figure 3b.

## 5. Conclusions

In conclusion, adapting a stochastic surface growth model to access the substrate sites sequentially, instead of randomly, can bring several advantages:

- Reduction of the short-time anomalies.
- Reduction of finite length effects.

---

<sup>1</sup>By independent I mean having its own internal variables.

- Increase of  $t_{\times}$  (useful when studying the roughening process, but an inconvenience when studying the steady state.)
- Smaller substrates are required when estimating macroscopic properties.
- Efficient use of the cache memory.
- Parallelizable algorithm.

It was shown that the reduction in the short-time anomalies is a consequence of changing the site selection from random to sequential. It cannot be explained by other differences between the models, like the change in the algorithm or the unfolding of one iteration of the RSE in to  $2d+1$  iteration of RRE and RSRRE. A possible explanation is the uniform surface scanning in the new model, while in the original model, a give site may, for example, not be updated for several units of time.

Not all surface growth models can be converted to perform sequential scanning. The etching model had to be altered to have only one modifiable site at each algorithm step, otherwise, the sweeping order will affect the dynamics. Furthermore, sequentializing is not possible if the rule applied in each cell is uniquely determined by the surface state, i.e., the rule must have some randomness. The surface width evolution was barely affected by that change, but was significantly altered by changing the order, from random to sequential, by which the substrate sites were accessed.

Two undesired aspects of the RRE as compared to the RSE are the use of twice as much memory and the division of the original step in  $2d+1$  steps which must be performed to achieve the same time evolution. However the changes pay off in light of the benefits: increased processing speed for big substrates and reduced short-time anomalies and finite size effect in small and big substrates.

## References

- [1] B. A. Mello, A. S. Chaves, F. A. Oliveira, Discrete atomistic model to simulate etching of a crystalline solid, *Phys. Rev. E* 63 (2001) 041113.
- [2] M. J. Vold, A numerical approach to the problem of sediment volume, *J. Coll. Sci.* 14 (1959) 168–174.
- [3] M. Eden, A two-dimensional growth process, in: *Proc. Fourth Berkeley Symp. on Math. Statist. and Prob.*, Vol. 4, 1961.
- [4] F. Family, Scaling of rough surfaces: effects of surface diffusion, *J. Phys. A* 19 (1986) L441.
- [5] J. M. Kim, J. M. Kosterlitz, Growth in a restricted solid-on-solid model, *Phys. Rev. Lett.* 62 (1989) 2289–2292.
- [6] R. Baiod, D. Kessler, P. Ramanlal, L. Sander, R. Savit, Dynamical scaling of the surface of finite-density ballistic aggregation, *Phys. Rev. A* 38 (1988) 3672–3679.



- [7] F. D. A. Aarão Reis, Dynamic transition in etching with poisoning, *Phys. Rev. E* 68 (2003) 041602.
- [8] F. D. A. Aarão Reis, Universality in two-dimensional kardar-parisi-zhang growth, *Phys. Rev. E* 69 (2004) 021610.
- [9] A. P. Reverberi, A. G. Bruzzone, L. Maga, A. Barbucci, Monte carlo simulation of a ballistic selective etching process in (2+1) dimensions, *Physica A* 354 (2005) 323–332.
- [10] F. D. A. Aarão Reis, Numerical study of roughness distributions in non-linear models of interface growth, *Phys. Rev. E* 72 (2005) 032601.
- [11] S. Kimiagar, G. R. Jafari, M. R. R. Tabar, Markov analysis and kramers-moyal expansion of the ballistic deposition and restricted solid-on-solid models, *J. Stat. Mech.-Theory E* (2008) P02010.
- [12] T. J. Oliveira, F. D. A. Aarão Reis, Maximal- and minimal-height distributions of fluctuating interfaces, *Phys. Rev. E* 77 (2008) 041605.
- [13] G. Tang, Z. Xun, R. Wen, K. Han, H. Xia, D. Hao, W. Zhou, X. Yang, L. Chen, Discrete growth models on deterministic fractal substrate, *Physica A* 389 (2010) 4552–4557.
- [14] Z. Xun, Y. Zhang, Y. Li, H. Xia, D. Hao, G. Tang, Dynamic scaling behaviors of the discrete growth models on fractal substrates, *J. Stat. Mech.-Theory E* (2012) P10014.
- [15] Z. Yong-Wei, T. Gang, H. Kui, X. Zhi-Peng, X. Yu-Ying, L. Yan, Numerical simulations of dynamic scaling behavior of the etching model on fractal substrates, *Acta Phys. Sin.* 61 (2012) 020511.
- [16] X. Yu-Ying, T. Gang, X. Zhi-Peng, H. Kui, X. Hui, H. Da-Peng, Z. Yong-Wei, L. Yan, Numerical simulation of dynamic scaling behavior of the etching model on randomly diluted lattices, *Acta Phys. Sin.* 61 (2012) 070506.
- [17] F. Family, T. Vicsek, Scaling of the active zone in the eden process on percolation networks and the ballistic deposition model, *J. Phys. A* 18 (1985) L75.
- [18] R. Jullien, R. Botet, Scaling properties of the surface of the eden model in  $d=2, 3, 4$ , *Journal of Physics A: Mathematical and General* 18 (1985) 2279.
- [19] K. A. Takeuchi, M. Sano, Universal fluctuations of growing interfaces: Evidence in turbulent liquid crystals, *Phys. Rev. Lett.* 104 (2010) 230601.
- [20] T. Sasamoto, H. Spohn, One-dimensional kardar-parisi-zhang equation: An exact solution and its universality, *Phys. Rev. Lett.* 104 (2010) 230602.

- [21] P. Calabrese, P. Le Doussal, Exact solution for the kardar-parisi-zhang equation with flat initial conditions, *Phys. Rev. Lett.* 106 (2011) 250603.
- [22] T. Imamura, T. Sasamoto, Exact solution for the stationary kardar-parisi-zhang equation, *Phys. Rev. Lett.* 108 (2012) 190603.
- [23] T. Halpin-Healy, (2+1)-dimensional directed polymer in a random medium: Scaling phenomena and universal distributions, *Phys. Rev. Lett.* 109 (2012) 170602.
- [24] T. J. Oliveira, S. G. Alves, S. C. Ferreira, Kardar-parisi-zhang universality class in  $(2 + 1)$  dimensions: Universal geometry-dependent distributions and finite-time corrections, *Phys. Rev. E* 87 (2013) 040102.
- [25] S. G. Alves, T. J. Oliveira, S. C. Ferreira, Universality of fluctuations in the kardar-parisi-zhang class in high dimensions and its upper critical dimension, *Phys. Rev. E* 90 (2014) 020103.
- [26] L. Moriconi, M. Moriconi, Conformal invariance in  $(2 + 1)$ -dimensional stochastic systems, *Phys. Rev. E* 81 (2010) 041105.
- [27] A. A. Saberi, M. D. Niry, S. M. Fazeli, M. R. Rahimi Tabar, S. Rouhani, Conformal invariance of isoheight lines in a two-dimensional kardar-parisi-zhang surface, *Phys. Rev. E* 77 (2008) 051607.
- [28] F. D. A. Aarão Reis, Universality and corrections to scaling in the ballistic deposition model, *Phys. Rev. E* 63 (2001) 056116.
- [29] S. V. Ghaisas, Stochastic model in the kardar-parisi-zhang universality class with minimal finite size effects, *Phys. Rev. E* 73 (2006) 022601.
- [30] J. Sanders, E. Kandrot, *CUDA by Example: An Introduction to General-Purpose GPU Programming*, Addison-Wesley Professional, 2010.
- [31] OpenMP Application Program Interface, OpenMP Architecture Review Board, 2013.   
arXiv:<http://www.openmp.org/mp-documents/OpenMP4.0.0.pdf>.
- [32] B. Chapman, G. Jost, R. van der Pas, *Using OpenMP: Portable Shared Memory Parallel Programming*, Scientific Computation Series, MIT Press, 2008.